

Climate-based approach for modeling the distribution of montane forest vegetation in Taiwan

Huan-Yu Lin^{1,2,3}  | Ching-Feng Li^{4,†}  | Tze-Ying Chen^{3,5}  | Chang-Fu Hsieh^{1,3}  |
Guangyu Wang⁶  | Tongli Wang⁷  | Jer-Ming Hu^{1,8} 

¹Institute of Ecology and Evolutionary Biology, National Taiwan University, Taipei, Taiwan

²Taiwan Forestry Research Institute, Taipei, Taiwan

³Biodiversity Association of Taiwan, Yilan City, Taiwan

⁴School of Forestry and Resource Conservation, National Taiwan University, Taipei, Taiwan

⁵Department of Forestry and Natural Resources, National Ilan University, Yilan City, Taiwan

⁶Department of Forest Resources, University of British Columbia, Vancouver, BC, Canada

⁷Department of Forest and Conservation Science, University of British Columbia, Vancouver, BC, Canada

⁸TAI Herbarium, National Taiwan University, Taipei, Taiwan

Correspondence

Jer-Ming Hu, Institute of Ecology and Evolutionary Biology, National Taiwan University, 1 Roosevelt Rd., Section 4, Taipei 106, Taiwan.
Email: jmhu@ntu.edu.tw

Funding information

Taiwan Forestry Bureau, research grant "A study on the resilience of biodiversity under long-term climate change," to HYL, TYC and CFH, Grant/Award Number: 106AS-11.7.1-FB-e1; Ministry of Science and Technology, Grant/Award Number: MOST 108-2621-B-002-004-MY3; Asia-Pacific Network for Sustainable Forest Management and Rehabilitation (APFNet) and the University of British Columbia, Grant/Award: "Adaptation of Asia-Pacific Forests to Climate Change Phase II," to HYL and TYC.

Abstract

Aims: Climate shapes forest types on our planet and also drives the differentiation of zonal vegetation at regional scale. A climate-based ecological model may provide an effective alternative to the traditional approach for assessing limitations, thresholds, and the potential distribution of forests. The main objective of this study is to develop such a model, with a machine-learning approach based on scale-free climate variable estimates and classified vegetation plots, to generate a fine-scale predicted vegetation map of Taiwan, a subtropical mountainous island.

Location: Taiwan.

Methods: A total of 3,824 plots from 13 climate-related forest types and 57 climatic variable estimates for each plot were used to build an individual ecological niche model for each forest type with random forest (RF). A predicted vegetation map was developed through the assemblage of RF predictions for each forest type at the spatial resolution of 100 m. The accuracy of the ensemble RF model was evaluated by comparing the predicted forest type with its original classification by plot.

Results: The climate environment of regions higher than 100 m above sea level in Taiwan was classified into potential habitats of 13 forest types by using model predictions. The predicted vegetation map displays a distinct altitudinal zonation from subalpine to montane cloud forests, followed by the latitudinal differentiation of subtropical mountain forests in the north and tropical montane forests in the south, with an average mismatch rate of 6.59%. An elevational profile and 3D visualization demonstrate the excellence of the model in estimating a fine, precise, and topographically corresponding potential distribution of forests.

Conclusions: The machine-learning approach is effective for handling a large number of variables and to provide accurate predictions. This study provides a statistical procedure integrating two sources of training data: (a) the locations of field sampling plots; and (b) their corresponding climate variable estimates, to predict the potential distribution of climate-related forests.

†Deceased 29 November 2019

KEYWORDS

climate, eastern Asia, ecological niche modeling, montane forest, random forest, subtropical forest, Taiwan, vegetation mapping

1 | INTRODUCTION

Climate is the primary element that governs the distribution of plant species, and most species are adapted to a specific range of climatic conditions, which is referred to as their climatic niche (Pearson & Dawson, 2003; Wang, Wang, Innes, Nitschke, & Kang, 2016). The vegetation–climate relationship has long been recognized by ecologists, and the concept has been applied to depict the regionalization of ecoregions or vegetation types for decades (Holdridge, 1947; Bailey, 1983; Su, 1984b; Fang, Song, Liu, & Piao, 2002). Recent progress in ecological niche modeling and the accessibility of accurate and fine-scale climate data has enabled vegetation–climate relationships to be used in numerous studies for a variety of purposes, including projection of the historical and current distribution of biomes and forests for management purposes (Rehfeldt, Crookston, Warwell, & Evans, 2006), prediction of changes in species (Matsui et al., 2018) or ecosystems (Brinkmann, Patzelt, Schlecht, & Buerkert, 2011; Rehfeldt, Crookston, Sáenz-Romero, & Campbell, 2012; Wang, Campbell, O'Neill, & Aitken, 2012) under various global warming scenarios, and provision of strategic tools for conservation and adaptation to the impact of climate change (Hansen & Phillips, 2015; Klassen & Burton, 2015; Wang, Wang, et al., 2016).

Most predictive ecological niche-modeling studies focused on large landscapes and dominant forests in temperate zones, but these studies seldom explored the complex, highly mixed, and species-diverse forests in tropical and subtropical regions. Distinguishing the boundaries of tropical and subtropical forest communities is difficult due to their similar broad-leaved physiognomy and variable composition (Zhu, Yong, Zhou, Wang, & Yan, 2015). Comprehensively and clearly tagged samples are requisite for training an effective and robust statistical classifier; however, the lack of high-quality field inventory data and the variable species composition in tropics and subtropics greatly limited the performance of statistical models in these extensive territories (Martin, Sherman, & Fahey, 2007).

Taiwan is an island located in the middle of the monsoon region of Asia with more than 200 peaks over 3,000 m a.s.l. The diverse climatic conditions along the altitudinal gradient create a distinct altitudinal zonation of forests within the island, from tropical lowland rainforest (Chao et al., 2010) to subalpine coniferous forest (Lin et al., 2012). The overall vegetation patterns on the island have been studied over the past few decades, recognizing and characterizing six distinct altitudinal vegetation zones within mesic to humid habitats (Su, 1984b). A national vegetation inventory was completed by the Taiwan Forestry Bureau in 2008. This inventory revealed that 58% of Taiwan's territory was covered by forests, 53% of which are broad-leaved forests, with the remaining approximately 47% of the forested lands comprised of coniferous or mixed forests. Li et al. (2013) established a vegetation classification scheme based on the floristic data of 8,804 plots from

the National Vegetation Database of Taiwan, which included 922 tree and shrub species in the analysis. They used the Cocktail determination key (CoDeK), a software application to formalize classification definitions, and developed automatic assignments of new plots to the defined vegetation classification scheme. Based on the formalized approach, a total of 6,574 plots were successfully classified into 21 forest types in which 12 types were zonal while nine types were azonal. Li et al. (2013) suggested that the main factors responsible for the differentiation of zonal forests are temperature and moisture, which vary according to the latitudinal distribution and altitudinal stratification in mesic to humid habitats. In contrast, most azonal forests are affected by specific soil properties or disturbance rather than climate, and their habitats are usually warmer and drier or colder and wetter than those of zonal forests.

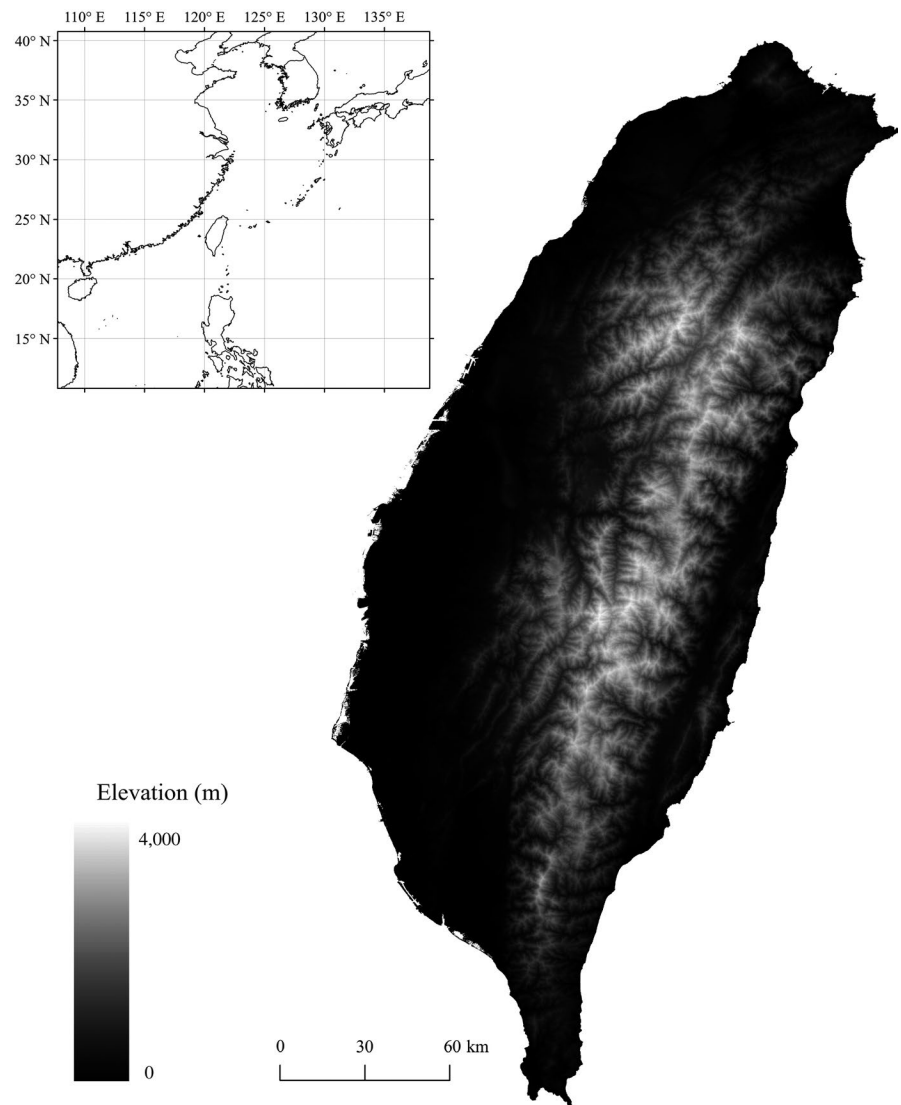
Since climate is the main factor controlling the differentiation of zonal vegetation, precise and fine-scaled climate data are considered to be a reasonable alternative for assessing limitations, thresholds, and the potential distribution of forests across a large landscape, if an effective statistical classifier exists. Machine learning is a new, high-performance approach applied in ecological niche modeling, which works outstandingly when a continuous supply of information for improving its performance is available. In Taiwan, intensive sampling plots tagged by the classification scheme and its corresponding climate variable estimates would be ideal sources to train a machine-learning model for exploring the vegetation–climate relationship. The main objectives of this study were to: (a) reveal the climatic factors responsible for the current distribution of dominant forest types in Taiwan; (b) develop an effective and reproducible statistical model for predicting the potential distribution of climate-related forests; and (c) use Taiwan's zonal vegetation as an example to evaluate the performance of the model.

2 | METHODS

2.1 | Study area

Taiwan (21.83–25.33° N, 120.00–122.00° E) is a subtropical island on the western edge of the Pacific Ocean. Hills and mountains occupy more than 70% of the island's 36,000 km². A principal mountain range, the Central Mountain Range, runs through the whole island in a NNE–SSW trend, and the highest peak is 3,952 m a.s.l. (Figure 1). The climate in Taiwan is mainly affected by the prevailing monsoons and typhoons. In winter, the northeast monsoon from Siberia passes through Japan and the East China Sea, bringing plentiful precipitation and cold temperature to the windward slopes of northeast Taiwan. By contrast, the southwest monsoon from Indochina and the South China Sea

FIGURE 1 Location and digital elevation surface of Taiwan island



brings heavy rains and a humid climate in the summer, inducing the rainy season in south Taiwan (Su, 1984a; Lin, Lung, Guo, Wu, & Su, 2009). Typhoons occur only occasionally but they represent severe climatic events in Taiwan. They contribute a sizable portion of the annual rainfall and are the primary trigger of landslides and disturbances in mountain areas.

Topographical variations in the form of lofty mountains and steep gorges result in a wide temperature range that forms distinct stratification of climatic zones in mountain areas and creates diverse microhabitats harboring many vascular plant species (~4,200 species). The zonation of forest types along the altitudinal gradient of Taiwan was first reported by Sasaki (1924), followed by a series of studies depicting the physiognomy and species composition of native flora (Suzuki, 1938; Liu & Su, 1972; Chang, 1974). Su (1984a, 1984b, 1985) evaluated overall vegetation patterns in Taiwan and concluded that the distribution of natural vegetation is governed by the alternating winter and summer monsoons, coupled with the steep topography. He also proposed a widely accepted scheme for classifying six altitudinal vegetation zones in mesic to humid habitats

and for some parts of the azonal vegetation in the drier successional regions of Taiwan.

2.2 | Vegetation data

The geographic coordinates of 6,574 plots and their corresponding 21 vegetation classification types were received from Li et al. (2013); then, a preliminary inspection was conducted to eliminate plots with duplicate coordinates. Eight forest types, which were climate-unrelated or geographically isolated, were removed from the original dataset: two types were seashore woodlands and mangroves; three types were successional woodland related to historical landslides and disturbances; two types were rock outcrop forests associated with uplifted coral-reef tableland, limestone, and scree slopes; and the last type was tropical forest on Green Island and Orchid Island, isolated from the Taiwan main island. Finally, a total of 3,824 plots belonging to 13 climate-related forest types (Table 1) were retained to explore the relationship between climate and vegetation.

TABLE 1 The training data incorporated in this study, including 13 climate-related forest types and their corresponding 3,824 field plots. The abbreviations of each forest type follows the classification by Li et al. (2013)

Forest type	Number of plots
High-mountain coniferous woodlands and forests (C1)	
<i>Juniperus</i> subalpine coniferous woodland and scrub (C1A01)	102
<i>Abies-Tsuga</i> upper-montane coniferous forest (C1A02)	89
Subtropical mountain zonal forests (C2)	
<i>Chamaecyparis</i> montane mixed cloud forest (C2A03)	543
<i>Fagus</i> montane deciduous broad-leaved cloud forest (C2A04)	55
<i>Quercus</i> montane evergreen broad-leaved cloud forest (C2A05)	1,058
<i>Machilus-Castanopsis</i> sub-montane evergreen broad-leaved forest (C2A06)	359
<i>Phoebe-Machilus</i> sub-montane evergreen broad-leaved forest (C2A07)	410
<i>Ficus-Machilus</i> foothill evergreen broad-leaved forest (C2A08)	145
Tropical mountain zonal forests (C3)	
<i>Pasania-Elaeocarpus</i> montane evergreen broad-leaved cloud forest (C3A09)	57
<i>Drypetes-Helicia</i> sub-montane evergreen broad-leaved forest (C3A10)	425
<i>Dysoxylum-Machilus</i> foothill evergreen broad-leaved forest (C3A11)	27
Tropical mountain azonal forests (C5)	
<i>Illicium-Cyclobalanopsis</i> tropical winter monsoon forest (C5A13)	40
Subtropical mountain azonal woodlands and forests (C6)	
<i>Pyrenaria-Machilus</i> subtropical winter monsoon forest (C6A15)	514
Total	3,824

2.3 | Climate data

Grid-based climate data were easily accessible and suitable for modeling general patterns at global and regional scales (Hannaway et al., 2005; Hijmans, Cameron, Parra, Jones, & Jarvis, 2005; Harris, Jones, Osborn, & Lister, 2014). However, for detailed ecological research, such climate data were usually too coarse to provide exact climate estimates for each plot in mountainous and topographically diverse areas. In Taiwan, a meteorological framework named the Taiwan Climate Change Projection and Information Platform (TCCIP) has integrated historical observations from thousands of weather stations to develop a 5 km × 5 km gridded climate surface covering the period of 1960–2012 (Hsu et al., 2011; Weng & Yang, 2012). A climate data downscaling process named *clim.regression* (Lin et al., 2018), which is based on a synthetic approach of bilinear interpolation and dynamic local regression (Wang, Hamann, Spittlehouse, & Carroll, 2016; Wang, Wang, Innes, Seely, & Chen, 2017), was used to downscale the TCCIP 5 km × 5 km dataset to a scale-free and seamless surface by conducting reasonable elevational adjustments using local lapse rate estimates. The accuracy of the climate downscaling model has been evaluated by comparing to historical observations from the 15 weather stations over different altitudinal zones. It demonstrated prediction errors of 0.56 °C, 0.79 °C, 0.80 °C, and 36.26 mm in T_{ave} , T_{min} , T_{max} , and PPT (measured by the mean absolute error between monthly estimation and observation), respectively, and these were considerably

improved over the TCCIP data (Lin et al., 2018). A total of 73 climate variable estimates were obtained through the downscaling process, including annual, seasonal, and monthly variables, alongside biologically relevant derivatives.

For exploring the relationship between vegetation and climate, 57 of the 73 climate variable estimates (Table 2), specific to the location of vegetation survey plots from Li et al. (2013) for the reference period of 1986–2005, were selected and were used as parameters to construct raw climate niche models for each forest type. Seasonal climate variables were not considered because of the large number of monthly variables. A gridded climate surface at a resolution of 100 m × 100 m, which covers regions higher than 100 m a.s.l. in Taiwan (2.7 million hectares in total), was generated from the same set of 57 climate variable estimates by *clim.regression* for predicting the climatic suitability of forests over the study area.

2.4 | Construction of the ecological niche model and vegetation prediction

The R version (Liaw & Wiener, 2002) of the random forest (RF) algorithm (Breiman, 2001) was used to model the relationship between the occurrence of each forest type and the climatic variables. RF works best when the samples are relatively balanced between classes (Breiman, 2001; Rehfeldt et al., 2006); however, most empirical classification problems and ecological samplings

TABLE 2 The 57 climate variables which were generated by the climate downscaling process of *clim.regression*, were incorporated in the random forest models

Climate variables	Definition
Monthly precipitation (PPT1 to PPT12)	
Mean annual precipitation (MAP)	
Mean summer precipitation (MSP)	Summation of precipitation from May to September
Ratio of winter precipitation (WPR)	$(PPT_{12} + PPT_{11} + PPT_{10}) / MAP$ (Li et al., 2013)
Mean monthly minimum temperature (T_{min1} to T_{min12})	
Mean monthly temperature (T_{ave1} to T_{ave12})	
Mean annual temperature (MAT)	
Mean monthly maximum temperature (T_{max1} to T_{max12})	
Temperature difference (TD)	T_{ave7} minus T_{ave1}
Annual heat:moisture index (AHM)	$(MAT + 10) / (MAP / 1000)$
Summer heat:moisture index (SHM)	$(T_{ave7}) / (MSP / 1000)$
Warmth index (WI)	Annual summation of mean monthly temperature higher than 5 °C (Su, 1984b)
Precipitation deficiency (PD)	Difference between annual potential evapotranspiration and MAP (Su, 1985)

are imbalanced. A total of 13 RF models, which represented the climatic niche of each forest type, were constructed in this study. For each RF model, plots belonging to the target forest type were treated as “presence,” and the remnants were regarded as “absence.” In most cases, occurrences of absence were much more common than those of presence for each forest type, leading to imbalanced samples, which can result in poor predictive performance for the minority (presence) class. Therefore, balanced random forest (Chen, Liaw, & Breiman, 2004) and multiple forest approaches (Wang, Wang, et al., 2016) were applied to build an ensemble of RF models to reduce the effect of imbalanced samples. Presence points (in minority) were combined with the same number of randomly selected points of absence (in majority), to establish the training dataset of each RF model. The identical sample size of absence and presence can ensure balanced sampling between classes. The above-mentioned model-building process was repeated 100 times to achieve “multiple forests” — the ensemble predictions from multiple forests were used to represent the climatic suitability of each forest type.

Although RF can handle confounding variables, a final model with the parsimonious set of variables that optimized variance is necessary to reduce the risk of over-fit and speed up the prediction. The R package VSURF was implemented to select a minimum set of predictors (Genuer, Poggi, & Tuleau-Malot, 2015) from the 57 climate variable estimates provided by *clim.regression* for each forest

Geographic cell	Climatic suitability of forest type				
	Type 1	Type 2	Type 3	...	Type n
Cell 1	P_{11}	P_{12}	P_{13}	...	P_{1n}
Cell 2	P_{21}	P_{22}	P_{23}	...	P_{2n}
...
Cell m	P_{m1}	P_{m2}	P_{m3}	...	P_{mn}

The projected forest type of cell k ($k = \{1, 2, 3, \dots, m\}$) was evaluated by the following workflow.

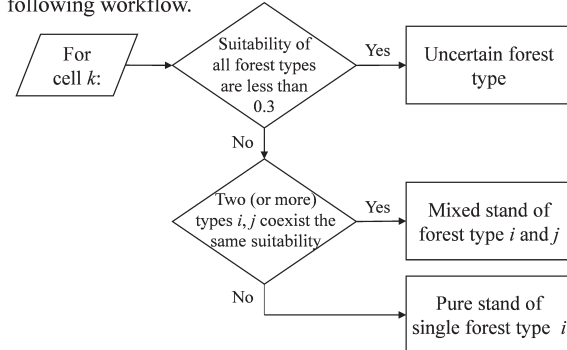


FIGURE 2 The workflow diagram for the ensemble of random forest (RF) predictions of each forest type to evaluate the most suitable forest type(s) of each geographic cell

type. VSURF first calculates the importance scores of all variables and eliminates variables of little importance, based on a descending importance rank. The variables that result in the lowest model out-of-bag (OOB) error are selected as explanatory variables. This set of explanatory variables is further truncated to eliminate all but one of any correlated variables, resulting in a minimum set of predictors for constructing the most parsimonious prediction model. For each simulation, we set the number of trees as 500 and used the default square root of the number of climate variables at each node (Liaw & Wiener, 2002).

Each geographical cell of the 100 m × 100 m projecting surface received climatic suitability for the 13 forest types based on predictions from multiple forests. Figure 2 presents a flow diagram evaluating the most suitable forest type for each cell according to the following criteria: (a) cells with climatic suitability lower than 0.3 for all forest types were classified as “uncertain”; (b) cells that shared the same suitability for two (or more) forest types (e.g., forest type i and j) and had suitability higher than 0.3 (included) were assigned as “mixed stands” between forest type i and j ; and (c) the remnant cells, namely those with high suitability for a single forest type, were defined as “pure stands” of the predicted forest type. The cut-off threshold of 0.3 in the first step affects the proportion of the study areas being identified as an “uncertain” entity. We tested values between 0 and 0.5 as the threshold and found a slight difference in resulting areas as type “uncertain,” ranging from 0 to 1,418 ha (accounting for 0–0.05% of the total study area). Thus, we arbitrarily chose the midpoint value 0.3 as the threshold, which demonstrates a performance similar to our field experience. The ensemble of climatic suitable forest types and their suitability were composed as a raster layer to produce the predicted vegetation map using ESRI ArcGIS Pro 2.4.

TABLE 3 The most parsimonious random forest (RF) model for each forest type through the variable selection process of VSURF package. Predictor variables were sorted by their importance (Gini values) in descending order

Forest type	Predictor variable/proportion of variable importance	OOB error rate (%)
<i>Juniperus</i> woodland and scrub	$T_{\max}6$ (37.6%), $T_{\max}5$ (34.2%), $T_{\max}3$ (15.3%), $T_{\max}4$ (12.9%)	1.2
<i>Abies-Tsuga</i> forest	$T_{\max}5$ (23.6%), $T_{\max}6$ (22.9%), $T_{\max}3$ (20.1%), $T_{\max}4$ (10.1%), $T_{\max}2$ (7.3%), $T_{\max}1$ (3.9%)	6.0
<i>Chamaecyparis</i> cloud forest	$T_{\max}12$ (19.9%), $T_{\max}2$ (13.1%), $T_{\max}1$ (8.2%), $T_{\max}9$ (8.1%), $T_{\max}6$ (5.5%), PPT12 (5.4%), $T_{\max}11$ (5.2%), PPT1 (5.0%), TD (4.7%), $T_{\max}2$ (3.8%), PPT11 (3.7%), WPR (3.5%), PPT6 (3.0%), WI (2.6%), $T_{\max}3$ (2.5%), $T_{\max}12$ (2.3%), PPT10 (1.8%), PPT3 (1.7%)	8.7
<i>Fagus</i> cloud forest	$T_{\max}12$ (21.6%), $T_{\max}2$ (19.8%), $T_{\max}1$ (18.6%), TD (11.9%), PPT1 (8.1%), $T_{\max}11$ (8.1%), PPT9 (7.6%), WPR (4.3%)	3.4
<i>Quercus</i> cloud forest	$T_{\max}6$ (14.1%), $T_{\min}12$ (13.4%), $T_{\max}6$ (10.2%), $T_{\min}10$ (9.6%), $T_{\max}7$ (8.2%), $T_{\max}2$ (6.7%), PPT1 (5.6%), PPT12 (5.2%), PPT3 (5.0%), PPT9 (4.6%), PPT10 (4.6%), $T_{\max}5$ (3.3%), $T_{\min}6$ (2.8%), $T_{\max}8$ (2.7%), PPT11 (2.4%), PPT6 (1.8%)	11.0
<i>Machilus-Castanopsis</i> forest	$T_{\max}4$ (15.9%), $T_{\max}10$ (13.6%), $T_{\max}11$ (10.8%), $T_{\min}6$ (9.9%), $T_{\max}6$ (7.9%), $T_{\max}5$ (7.2%), $T_{\max}3$ (7.1%), PPT10 (6.6%), $T_{\max}12$ (6.4%), $T_{\max}1$ (4.9%), $T_{\max}9$ (4.1%), $T_{\max}7$ (2.8%), PPT8 (2.7%)	16.7
<i>Phoebe-Machilus</i> forest	$T_{\max}9$ (18.7%), $T_{\max}2$ (15.1%), $T_{\max}7$ (12.4%), PPT3 (10.8%), PPT7 (8.6%), PPT4 (8.3%), $T_{\max}11$ (8.0%), $T_{\max}9$ (7.3%), TD (2.9%), PPT9 (2.8%), PPT8 (2.6%), PPT10 (2.5%)	18.2
<i>Ficus-Machilus</i> forest	$T_{\max}11$ (26.1%), $T_{\max}10$ (25.9%), $T_{\max}9$ (13.9%), SHM (12.1%), $T_{\max}8$ (11.6%), AHM (1.3%), MSP (3.1%), PPT5 (3.0%)	5.2
<i>Pasania-Elaeocarpus</i> cloud forest	PPT4 (34.4%), PPT2 (26.4%), PPT3 (20.5%), WPR (9.1%), $T_{\max}9$ (5.0%), PPT7 (4.5%)	6.8
<i>Drypetes-Helicia</i> forest	PPT3 (42.7%), PPT2 (16.0%), TD (13.6%), $T_{\max}1$ (10.8%), PPT1 (6.6%), $T_{\max}8$ (6.5%), PPT8 (3.9%)	5.7
<i>Dysoxylum-Machilus</i> forest	$T_{\max}2$ (45.7%), $T_{\max}1$ (40.4%), PPT5 (13.8%)	7.0
<i>Illicium-Cyclobalanopsis</i> winter monsoon forest	PPT4 (43.2%), $T_{\min}1$ (31.6%), TD (25.1%)	5.6
<i>Pyrenaria-Machilus</i> winter monsoon forest	TD (48.1%), PPT11 (28.1%), PPT1 (15.1%), PPT12 (8.6%)	6.8

3 | RESULTS

3.1 | Climatic niche and important variables of forest types

The result of VSURF variable truncation revealed that the importance and number of selected climate variables varied among forest types. The OOB error arising from the model-building process of 500 trees is 7.9% on average, ranging from 1.2% to 18.2% depending on forest type (Table 3). The vegetation-climate relationships of high-mountain and subtropical mountain zonal forests (from *Juniperus* woodland and scrub to *Ficus-Machilus* forest in Table 3) are strongly driven by temperature factors (T_{\max} , T_{\max} , and T_{\min}); that is, the primary predictors of high-mountain, temperate, and subtropical forests are usually dominated by temperature rather than precipitation, respectively. Furthermore, the maximum monthly temperature at the start of the growing season (March to June) closely relates to the occurrence of subalpine and coniferous forests (*Juniperus* and *Abies-Tsuga*) distributed at elevations higher than 2,500 m a.s.l. The critical effect shifts to winter temperature (December to February) for cloud forests at elevations of 1,500–2,500 m a.s.l., which are dominated by *Chamaecyparis* or *Fagus*. By contrast, precipitation-related factors, especially

the relative dryness in spring (March to May), display a more evident correlation with the climatic suitability of tropical mountain zonal forests in south Taiwan (*Pasania-Elaeocarpus* cloud forest, *Drypetes-Helicia* forest, and *Dysoxylum-Machilus* forest). Due to the co-effect of topographical exposure and windward chilling of the northeast monsoon during winter, two azonal forest types, the tropical *Illicium-Cyclobalanopsis* monsoon forest and the subtropical *Pyrenaria-Machilus* monsoon forest, exhibit climatic features of higher precipitation and lower temperature than habitats nearby them in winter (Figure 3 and Appendix S1).

3.2 | Predicted vegetation map

A predicted vegetation map was obtained based on the ensemble of predictions from multiple forests. Climate environment of the entire study area was classified into potential habitats of 13 forest types (Figure 4). The predicted map displays an obvious altitudinal zonation from high-mountain woodland to montane cloud forests, followed by the latitudinal differentiation of sub-montane and foothill forests in the subtropical and tropical parts of Taiwan. Two azonal forests, the tropical *Illicium-Cyclobalanopsis* forest and the subtropical *Pyrenaria-Machilus* forest, are mapped in the southern peninsula

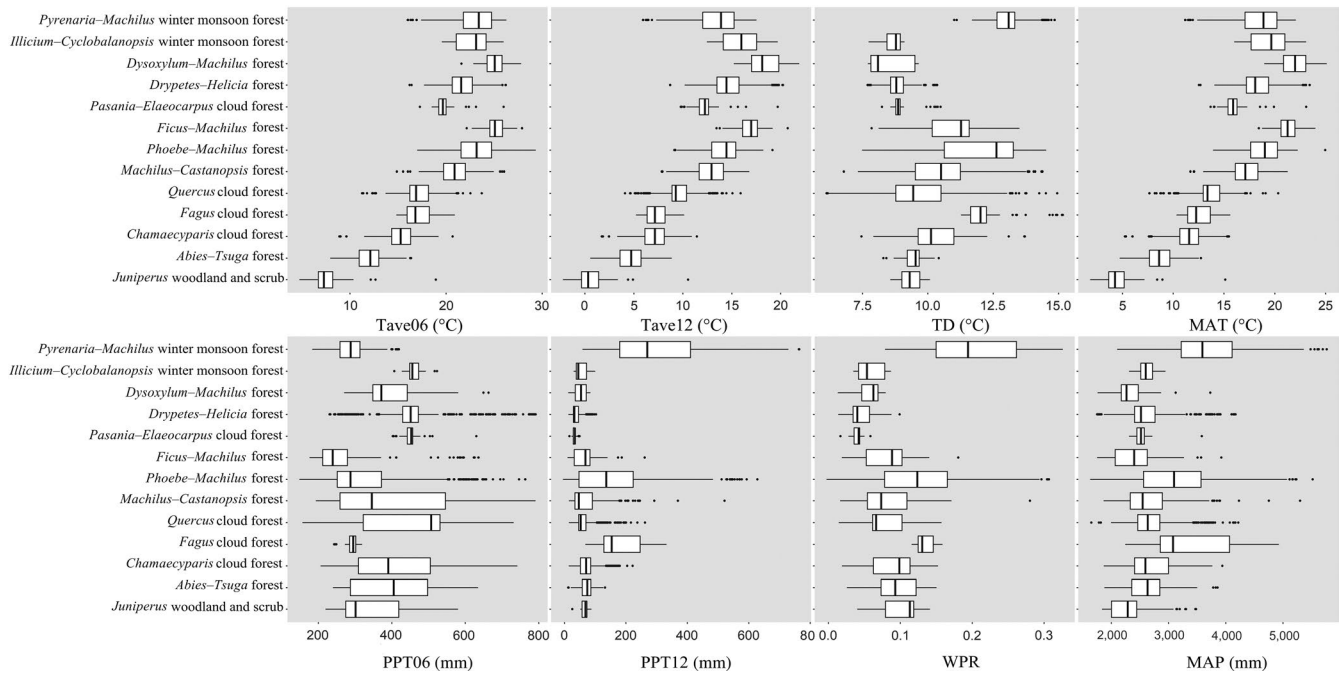


FIGURE 3 Range of climatic variable estimates on the location of sampling plots of each forest type

and the northeast corner. *Ficus-Machilus* forest is the most widespread vegetation, occupying 25.64% of Taiwan's slope land. The rank of occupying area is followed by *Quercus* cloud forest (13.22%), *Machilus-Castanopsis* (12.05%), and *Phoebe-Machilus* forest (11.74%). High-mountain habitats with a total area of 390,000 ha, which are suitable for coniferous woodland and forests such as *Juniperus*, *Abies*, *Tsuga*, and *Chamaecyparis*, account for 14.52% of the study area. The area of habitats suitable for tropical mountain zonal forests is close to that for high-mountain vegetation (390,000 ha, accounting for 14.49%) but distribution is relatively sparse among the predicted regions (Table 4).

The altitudinal distribution of forests showed that most forest types dominate in a distinct altitudinal range (Figure 5); for example, *Juniperus* woodland and scrub occupied a mean elevation of 3,078 m a.s.l., *Abies-Tsuga* forest at 2,743 m a.s.l., *Chamaecyparis* cloud forest at 2,274 m a.s.l., and *Pasania-Elaeocarpus* cloud forest at 1,657 m a.s.l. in southern Taiwan. However, the altitudinal ranges of some forest types are overlapping and mixed; for example, *Fagus* cloud forest co-occurs with *Quercus* cloud forest at an elevation of 1,700 m a.s.l., *Machilus-Castanopsis* and *Phoebe-Machilus* forests are generally co-dominant at elevations of 800–1,000 m a.s.l., and two foothill forest types, *Ficus-Machilus* and *Dysoxylum-Machilus* forests, are mixed at elevations of 200–300 m a.s.l. in southern Taiwan (Figure 5).

The workflow of Figure 2 depicts the core region of each forest type and indicates habitats where adjacent forest types coexisted. The ensemble of multiple forests predicted that 72.67% of the study area (1,970,000 ha) was climatically suitable for a single dominant forest type, classified as a pure stand. However, the climatic environment of 730,000 ha (~27.33% of the study area) was predicted to be suitable for two or more coexisting forest types, classified as a mixed stand. The remaining areas, 506 ha (0.02%),

could not be identified by the RF models and are classified as uncertain (Table 4). Figure 6 shows examples illustrating the predicted pure stands and mixed stands in the high-mountain areas of north Taiwan (Figure 6a) and in the tropical low hills of south Taiwan (Figure 6b). Because of topographical influences on mesoclimate in the mountains, including lapse rate, orographic precipitation, and windward effects, the occurrence of mixed stands usually follows the iso-altitudinal belts on slopes. However, the spatial extent of the predicted mixed stands stretches from hundreds to thousands of meters in width, depending on mountain steepness, aspect, and climate variation. The *Ficus-Machilus* forest is the most widespread forest type but it also shares a broader area of mixed stands of 160,000 ha with other forests, 66% of which (~110,000 ha) are habitats mixed with *Dysoxylum-Machilus* forest, mainly distributed in the tropical lowland of Taiwan. The *Phoebe-Machilus* forest (130,000 ha in total), primarily occurring at a middle elevation of 800 m a.s.l., is another forest type which has 46% (~60,000 ha) of mixed stands with its upper neighboring *Machilus-Castanopsis* forest at the ranges of 850–1,000 m a.s.l.

3.3 | Statistical evaluation of the ensemble model

In addition to the OOB error assessed during the model-building process of each forest type, the overall accuracy of the ensemble RF models was evaluated by comparing the prediction at locations of the 3,817 forest type-classified plots (Table 5). Model errors of fit (mismatch rate) were low for most forest types, ranging from 1.96% to 17.50% with an average of 6.59%. The findings revealed that the performance of the RF model was lower for distinguishing three vegetation types, namely *Illicium-Cyclobalanopsis* winter monsoon forest (error = 17.50%),

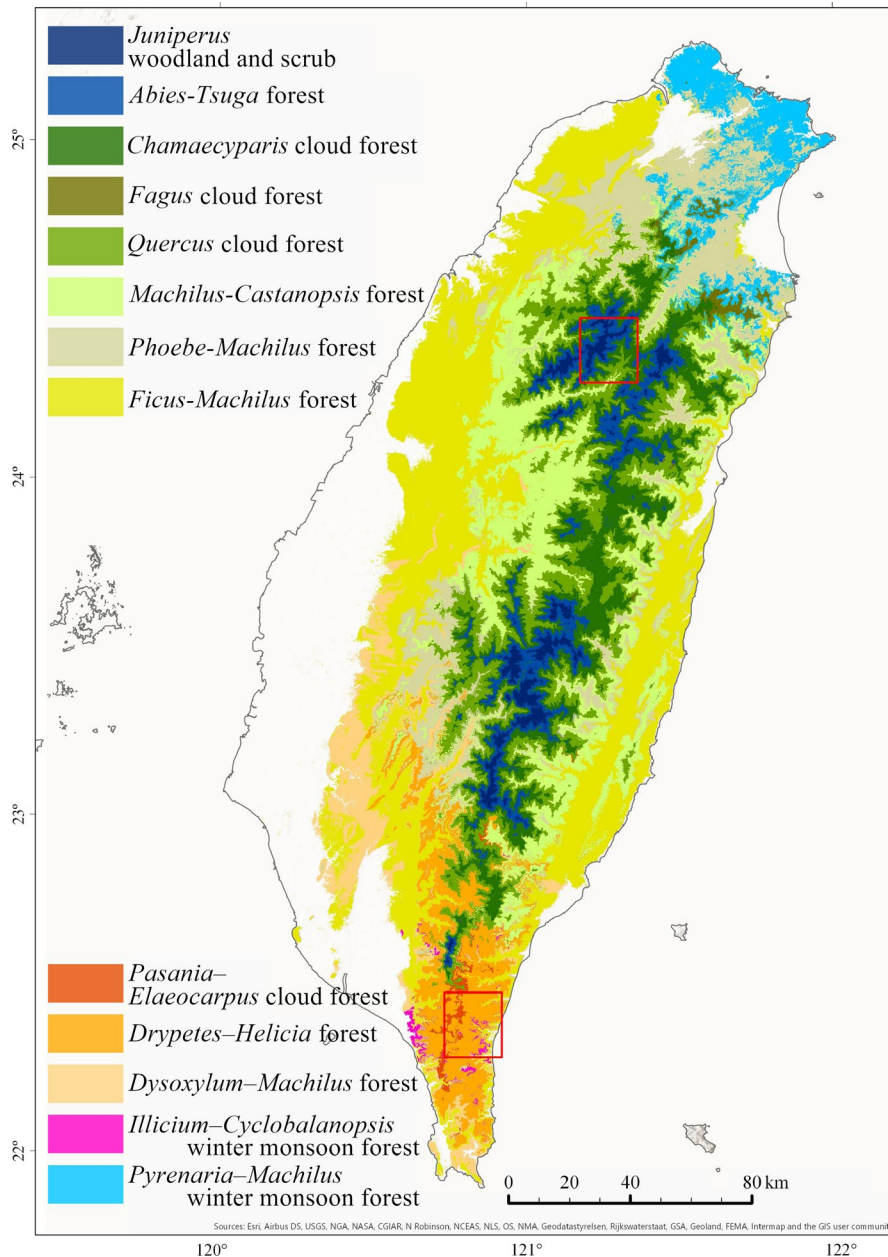


FIGURE 4 Predicted vegetation map of study area based on the ensemble of suitability of each forest type. The red rectangles are sample areas for illustrating the map in detail (see Figure 6)

Machilus-Castanopsis forest (error = 14.21%), and *Phoebe-Machilus* forest (error = 10.98%). These three forest types mainly occur at elevations from 479 to 1,030 m a.s.l., the altitudinal range where several vegetation types tend to coexist and form mixed stands in Taiwan (Figure 5).

4 | DISCUSSION

4.1 | Model accuracy and its ability to predict the potential distribution of forests

The Random Forests approach is an ensemble classifier that aggregates and averages predictions across multiple trees to generate robust outcomes. This method has been recommended for modeling the ecological niche of organisms and predicting their potential

distribution (Wang et al., 2012; Chiu et al., 2013; Zhang et al., 2015), and it has been widely applied on both regional and global scales for the use of conservation and adaptation to environmental change (Attorre et al., 2011; Rehfeldt et al., 2012, 2006; Wang, Wang, et al., 2016). In this study, RF models performed with a high degree of accuracy in predicting the potential distribution of forest vegetation in Taiwan, with a mismatch rate of 6.59% on average.

However, the prediction accuracy for several forest types is comparatively lower, such as *Illicium-Cyclobalanopsis* winter monsoon forest (with a mismatch rate of 17.50%), *Machilus-Castanopsis* forest (14.21%), and *Phoebe-Machilus* forest (10.98%). Several possible reasons for this result are as follows: (a) *Illicium-Cyclobalanopsis* forest is tropical vegetation exposed to winter monsoon directly, which is characterized by its cold-humid climate during winter, the high stem density, and richness in sclerophyllous

**TABLE 4** The area statistics of predicted forest types, pure stands and mixed stands are included

Predicted forest type	Total area (ha)	%	Pure stand		Mixed stand		Coexisting forest type(s) within mixed stands and its proportion
			Area (ha)	%	Area (ha)	%	
<i>Juniperus</i>	29,134	1.08	13,590	46.65	15,544	53.35	<i>Abies-Tsuga</i> (1.00)
<i>Abies-Tsuga</i>	114,151	4.21	76,930	67.39	37,221	32.61	<i>Juniperus</i> (0.42), <i>Chamaecyparis</i> (0.58)
<i>Chamaecyparis</i>	250,006	9.23	204,420	81.77	45,586	18.23	<i>Abies-Tsuga</i> (0.47), <i>Fagus</i> (0.04), <i>Quercus</i> (0.49)
<i>Fagus</i>	15,433	0.57	9,993	64.75	5,440	35.25	<i>Chamaecyparis</i> (0.30), <i>Quercus</i> (0.06), <i>Pyrenaria-Machilus</i> (0.64)
<i>Quercus</i>	358,009	13.22	322,318	90.03	35,691	9.97	<i>Chamaecyparis</i> (0.62), <i>Fagus</i> (0.01), <i>Machilus-Castanopsis</i> (0.24), <i>Phoebe-Machilus</i> (0.04), <i>Pasania-Elaeocarpus</i> (0.02), <i>Pyrenaria-Machilus</i> (0.07)
<i>Machilus-Castanopsis</i>	326,277	12.05	233,338	71.52	92,939	28.48	<i>Quercus</i> (0.09), <i>Phoebe-Machilus</i> (0.65), <i>Ficus-Machilus</i> (0.14), <i>Pasania-Elaeocarpus</i> (0.01), <i>Drypetes-Helicia</i> (0.07), <i>Pyrenaria-Machilus</i> (0.04)
<i>Phoebe-Machilus</i>	318,017	11.74	185,980	58.48	132,037	41.52	<i>Quercus</i> (0.02), <i>Machilus-Castanopsis</i> (0.46), <i>Ficus-Machilus</i> (0.28), <i>Drypetes-Helicia</i> (0.02), <i>Pyrenaria-Machilus</i> (0.22)
<i>Ficus-Machilus</i>	694,606	25.64	531,653	76.54	162,953	23.46	<i>Machilus-Castanopsis</i> (0.08), <i>Phoebe-Machilus</i> (0.23), <i>Drypetes-Helicia</i> (0.01), <i>Dysoxylum-Machilus</i> (0.66), <i>Illicium-Cyclobalanopsis</i> (0.02)
<i>Pasania-Elaeocarpus</i>	8,750	0.32	5,474	62.57	3,276	37.43	<i>Quercus</i> (0.19), <i>Machilus-Castanopsis</i> (0.01), <i>Ficus-Machilus</i> (0.02), <i>Drypetes-Helicia</i> (0.62), <i>Dysoxylum-Machilus</i> (0.11), <i>Illicium-Cyclobalanopsis</i> (0.05)
<i>Drypetes-Helicia</i>	143,575	5.30	111,772	77.85	31,803	22.15	<i>Machilus-Castanopsis</i> (0.20), <i>Phoebe-Machilus</i> (0.08), <i>Ficus-Machilus</i> (0.04), <i>Pasania-Elaeocarpus</i> (0.06), <i>Dysoxylum-Machilus</i> (0.20), <i>Illicium-Cyclobalanopsis</i> (0.42)
<i>Dysoxylum-Machilus</i>	240,205	8.87	122,659	51.06	117,546	48.94	<i>Ficus-Machilus</i> (0.91), <i>Drypetes-Helicia</i> (0.06), <i>Illicium-Cyclobalanopsis</i> (0.03)
<i>Illicium-Cyclobalanopsis</i>	27,314	1.01	8,096	29.64	19,218	70.36	<i>Ficus-Machilus</i> (0.17), <i>Pasania-Elaeocarpus</i> (0.01), <i>Drypetes-Helicia</i> (0.68), <i>Dysoxylum-Machilus</i> (0.14)
<i>Pyrenaria-Machilus</i>	182,806	6.75	142,180	77.78	40,626	22.22	<i>Fagus</i> (0.09), <i>Quercus</i> (0.06), <i>Machilus-Castanopsis</i> (0.12), <i>Phoebe-Machilus</i> (0.72), <i>Ficus-Machilus</i> (0.01)
Uncertain	506	0.02	–	–	–	–	
Total	2,708,789	100.00	1,968,403	72.67	739,880	27.33	

species. This forest type is narrowly restricted to windward hill ridges, but converts to high canopy leeward or to valley forests dramatically as the topography changes (Chao et al., 2010; Li et al., 2013). In southern Taiwan, the habitats of *Illicium-Cyclobalanopsis* forest are usually fragmented and form a mosaic with sub-montane and foothill forests such as *Drypetes-Helicia* forest, *Ficus-Machilus* forest, and *Dysoxylum-Machilus* forest. The transition of vegetation can occur over a very short distance, even <50 m (Chao, et al., 2007), which is too localized for the climate down-scaling model to detect, resulting in a high percentage of mixed stands and low accuracy in the RF predictions. (b) The other two

forest types with lower prediction accuracy, *Machilus-Castanopsis* forest and *Phoebe-Machilus* forest, are usually found at similar altitudinal ranges of 400–1,800 and 0–1,400 m (Li et al., 2013). At elevational ranges where *Machilus-Castanopsis* forest and *Phoebe-Machilus* forest co-occur, the former usually dominates on ridges with drier and well-developed soil, whereas the latter has a low abundance and frequency of Fagaceae and tends to occur in relatively narrow, shaded valleys, and humid habitats. The similarity in altitudinal ranges in combination with differentiation among microhabitats for *Machilus-Castanopsis* forest and *Phoebe-Machilus* forest may explain the lower prediction accuracy.

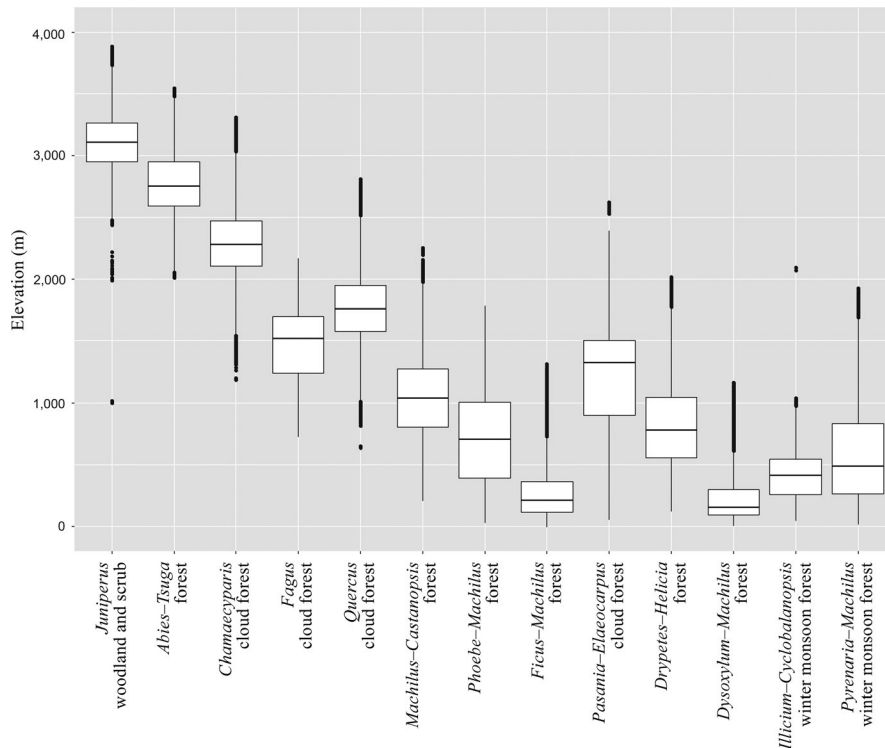


FIGURE 5 The altitudinal ranges of forests based on the predicted vegetation map. Core habitats of most forest types occupied distinct altitudinal regions, however, habitats of some forests (eg. *Fagus* & *Quercus*, *Machilus*–*Castanopsis* & *Phoebe*–*Machilus*, *Pasania*–*Elaeocarpus* & *Drypetes*–*Helicia*, *Ficus*–*Machilus* & *Dysoxylum*–*Machilus*) were partially overlapped in elevation

Although a machine-learning model is difficult to interpret due to its complex variables, it can provide a starting point for identifying key predictor variables and testing theory in an experimental framework. For example, our results show that temperature variables contribute to distinctly separate potential habitats of *Juniperus* woodland, *Abies-Tsuga*, *Chamaecyparis*, and *Fagus* forests (Table 3 and Appendix S1). Maximum monthly temperature of the growing season, especially at the thresholds of 15 °C (May) and 16.5 °C (June), closely corresponds with the boundaries of *Juniperus* woodland and *Abies-Tsuga* forest. For *Chamaecyparis* and *Fagus* forests, the important variables contributing to the RF model shift to winter temperature; for example, the thresholds of 7.2 °C (T_{ave} of December), 11.9 °C (T_{max} of February), 5.9 °C (T_{ave} of January) for *Chamaecyparis* forest; and monthly maximum temperatures of 12.4 °C (December), 11.6 °C (February), and 10.7 °C (January) for *Fagus* forest. The results also indicate that annual temperature difference (TD) and winter precipitation play important roles in identifying the potential habitat of *Fagus* from other forest types. The range and threshold of predictors from a machine-learning model can provide insight into ways of broader exploration in ecosystems and can lead to a better understanding of forest habitat differentiation.

4.2 | Detailed inspections of the RF model predictions

Gradients of the physical environment may result in the presence of varying organisms and communities, which can lead to directional changes in the composition, physiognomy, and biological

interactions of forests (Whittaker, 1975). A prominent niche model should elucidate factors that critically relate to biological phenomena, and precisely project these factors to their spatial extent.

In Taiwan, it has been reported that the mountain temperatures for a given elevation are higher at the central part of the mountain range, and lower at both the north and the south ends (Su, 1984a). This phenomenon may be attributed to the heat retention mechanism of Massenerhebung (Su, 1984a) or the cooling effect induced by the northeast monsoon (Chiou et al., 2010), and it is responsible for the altitudinal compression of vegetation zones at the northern and southern tips of Taiwan, while a most extensive and distinguishable zonation in the middle part can be found. This pattern can be simulated well by our approach. Figure 7 illustrates the north-south profiles on model predictions of seven selected forest types, which are widespread throughout Taiwan, and demonstrates evident downward compression of vegetation zones at the north and south ends while a more extensive altitudinal distribution was modeled in central Taiwan.

Except for the large-scale climate patterns, topo-climatic variations such as rain shadow, radiative difference, and windward cooling also influence the local distribution of forests. Snow Mountain is a mountain mass located in the middle of the northwest and central west climate region of Taiwan with the highest peak at an elevation of 3,886 m, where its northeast-facing slope is cool and humid due to the lack of sunlight and moist air brought by the winter monsoon, yet a relatively warm and dry environment is formed on its south slope (Su, 1985). Su (1984b) reported that similar vegetation types occurred at lower elevations on the north-facing slope, e.g. the *Abies* zone distributed at 2,600–3,100 m (north) vs

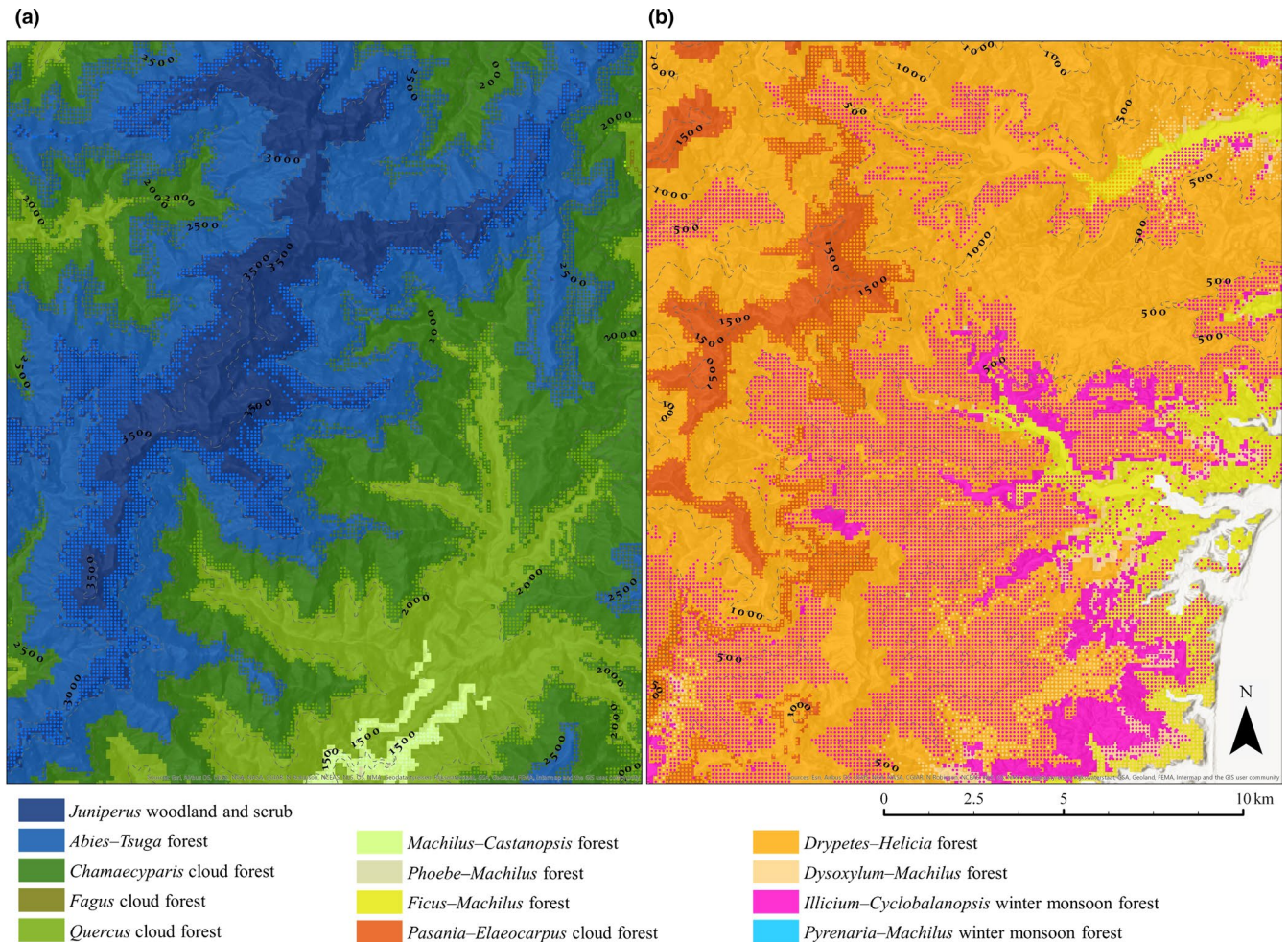


FIGURE 6 The detailed mapping of predicted forest types. A pure stand is represented by a single color, whereas a mixed stand is indicated by the coexistence of a dot. (a) The prediction of high-mountain and subtropical montane forests with types of *Juniperus*, *Abies-Tsuga*, *Chamaecyparis*, *Quercus*, and *Machilus-Castanopsis*. The belt-like mixed stands usually occur along an iso-elevation hillside. (b) The predicted mapping of tropical forests in southeast Taiwan where tropical montane forests (*Pasania-Elaeocarpus* and *Drypetes-Helicia*) mixed with subtropical foothill forest (*Ficus-Machilus*) and tropical winter monsoon forest (*Illicium-Cyclobalanopsis*). Broadly mixed stands of *Drypetes-Helicia* forest and *Illicium-Cyclobalanopsis* forest occurred at the north slope in a valley, where a cooler habitat exposed to the northeast monsoon during winter is predicted

2,900–3,400 m (south); the *Tsuga* zone at 2,200–2,800 m (north) vs 2,200–2,900 m (south); and the *Chamaecyparis* zone at 1,600–2,300 m (north) vs 1,700–2,400 m (south). We applied the RF models to predict and visualize the potential distributions of forests on Snow Mountain (Figure 6a and Appendix S2, or see the animation at <https://youtu.be/Nar76WVDp30>) and verified it with observations made by Su in 1984. The predicted forest distributions are in very close agreement with Su's observations. Based on the work diagram of Figure 2, the RF models also indicate the locations of mixed stands, which is analogous to the characteristic of an ecotone — a community comprising part of the ecological features of its neighbors but having a specific site characteristic of its own (Barnes, Zak, Denton, & Spurr, 1997; Holland & Risser, 1991). On Snow Mountain, for example, the models identified mixed stands, 400 m in width, between *Juniperus* woodland and *Abies-Tsuga* forest, and also mapped the transition between *Chamaecyparis* forest and *Quercus* forest.

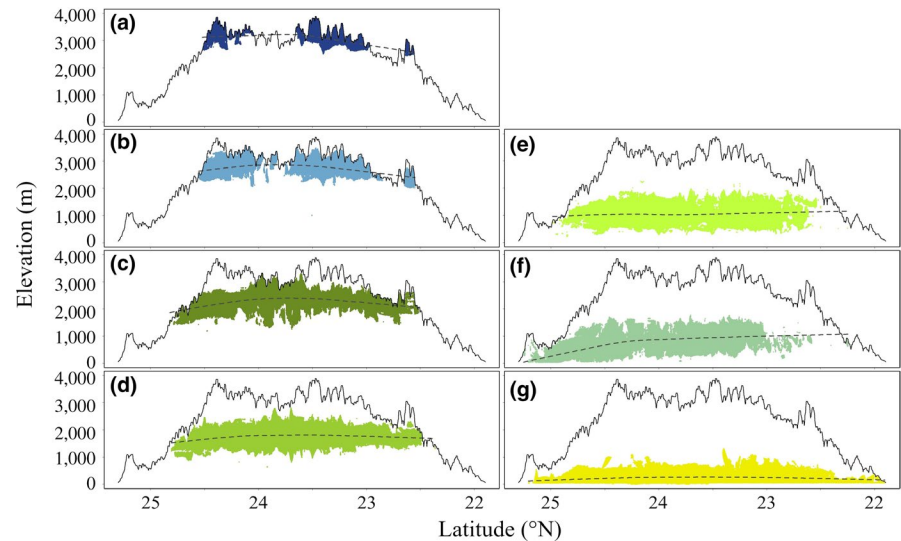
4.3 | Applications of the RF model

In recent decades, climate data have become available from various sources published at fine-scale resolutions for ecological studies (Hannaway et al., 2005; Hijmans et al., 2005; Harris et al., 2014). The results of several studies in Europe (Hengl et al., 2018), North America (Rehfeldt et al., 2012; Wang et al., 2012), and mainland China (Zhang et al., 2015; Wang, Wang, et al., 2016) suggest that RF modeling is one of the optimal approaches for niche modeling and species distribution prediction, when sufficient presence/absence data exist (Zhang et al., 2015; Hengl et al., 2018). Fine-resolution predictions are particularly suitable for local interpretation and decision-making applications. Most ecological niche-modeling studies have employed published global or regional climate databases, which have finest spatial resolutions of arc-seconds or kilometers, but they are still too coarse to provide detailed information regarding mountainous and topographically diverse areas.

TABLE 5 A confusion matrix of actual forest type vs predicted forest type for evaluating the accuracy of ensemble predictions. Seven plots are located outside the study area and eliminated from this evaluation

Predicted forest types															
J.	A.-T.	C.	F.	Q.	M.-C.	P.-M.	F.-M.	P.-E.	D.-H.	D.-M.	I.-C.	P.-M.	Number of samples	Mismatch (%)	
Actual forest types															
Juniperus	100	1		1									102	1.96	
Abies-Tsuga	82	7											89	7.87	
Chamaecyparis	4	511	3	22	1							2	543	5.89	
Fagus		1	53									1	55	3.64	
Quercus	3	32	3	992	14	3			10			1	1,058	6.24	
Machilus-		1	1	9	308	11	1		17	1	1	9	359	14.21	
Castanopsis															
Phoebe-Machilus				3	14	365	8		2		1	17	410	10.98	
Ficus-Machilus						1	141		1	1			144	2.08	
Pasania-								55	1		1		57	3.51	
Elaeocarpus															
Drypetes-Helicia				1	5		2	3	410	1	3		425	3.53	
Dysoxylum-									2	24			26	7.69	
Machilus															
Illicium-								4	3		33		40	17.50	
Cyclobalanopsis															
Pyrenaria-Machilus		1	1	1	1	14						491	509	3.54	
Outside													7	-	
Number of predictions	100	90	553	61	1,029	343	394	152	62	446	27	39	521	3,824	6.59

FIGURE 7 Simulated distributions of seven selected zonal forest types on the elevational profile. (a) *Juniperus* woodland and scrub; (b) *Abies-Tsuga* forest; (c) *Chamaecyparis* cloud forest; (d) *Quercus* cloud forest; (e) *Machilus-Castanopsis* forest; (f) *Phoebe-Machilus* forest; (g) *Ficus-Machilus* forest



Besides, species from adjacent zones may occur and coexist along the border of a given zone due to their close climatic suitability and ecological requirements. Because of the mixed, intermediate, and specific ecological characteristics of ecotones, they have been reported as important species-rich areas for influencing local and regional biodiversity patterns (Martin et al., 2007; Neilson, 1993). Inhabitants of ecotones are often near their physical limits and competitive tolerance, which means they may be sensitive to fluctuations and changes of environmental factors, and they are usually regarded as early indicators of the effects of climate change (Neilson, 1993; Risser, 1995; Wasson, Woolfolk, & Fresquez, 2013). The monitoring of migration patterns and compositional change in ecotones is one of the primary approaches for tracing the effects of climate change. For example, the range shift and demographical change of mountain forests often correspond with directional climatic change (Beniston, 2003; Beckage et al., 2008; Evans & Brown, 2017).

Taiwan is a relatively small continental island, where the interactions of humid monsoons, frequent typhoons, and dramatic topographical differences result in its diverse habitats and climatic conditions. The rainfall is enough for forest establishment over the whole island; however, factors including: (a) the significant temperature gradient along the elevational extent (Su, 1984b); (b) differences in seasonal precipitation (Su, 1985); and (c) mixed floras from tropical Asia and temperate Asia due to the island's historical and geographical context (Hsieh, Shen, & Yang, 1994), co-contribute to the diverse forests harboring plants from tropical, temperate, and even subarctic regions. We suggest that potential vegetation maps at high resolution can be powerful aids to serve as drafts for stand classification, guides for optimal land use, and fundamental models for projecting vegetation change under global warming scenarios. This study provides a statistical procedure integrating locations of field sampling plots and their corresponding climate variable estimates to calculate, simulate, and visualize the potential distribution of climate-related forests. These applications especially benefit regions with complicated landscape mosaics with highly differentiated vegetation communities, such as Taiwan. When detailed and

precise training data are applied, e.g. the updated historical climate observations, future climate change scenarios, or supplemented information from more field plots, this procedure is reproducible and can be used to update the predicted forest map for prompt use in resource management.

Last, we acknowledge that this study and its findings have several limitations. Azonal forests, whose occurrence and mortality are largely affected by non-climatic factors such as disturbances, succession, hydrologic regimes, and edaphic conditions, were not examined in detail. Although climate plays an important role in the distribution of zonal forests, there are still mechanical processes — such as competition, dispersal ability, and biotic or abiotic interactions — that are not considered by the statistical model in this study. Clearly, correlational modeling approaches can provide effective indications regarding ecological niches and potential distributions of organisms for the use in large-scale resource management, but non-climatic variables and mechanical processes should also be considered while conducting planning and management of natural resources at local scales.

ACKNOWLEDGEMENTS

The authors would like to thank the TCCIP for providing access to their data. The co-author, Dr. Ching-Feng Li, passed away during the preparation of this manuscript. We would like to take this opportunity to honor his contribution to vegetation ecology in Taiwan.

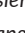


AUTHOR CONTRIBUTIONS

HYL and JMH conceived the research idea and led the writing; CFL, TYC, and CFH contributed the data and vegetation classification; HYL performed the statistical analyses with contributions from GW and TW; all authors discussed the results and commented on the manuscript.

DATA AVAILABILITY STATEMENT

The original data, occurrence of the 13 climate-related forest types and climatic parameters specific to the locality of each plot, can be found in Appendix S3.

ORCID

Huan-Yu Lin  <https://orcid.org/0000-0002-7340-0713>
 Ching-Feng Li  <https://orcid.org/0000-0003-0744-490X>
 Tze-Ying Chen  <https://orcid.org/0000-0001-5842-1834>
 Chang-Fu Hsieh  <https://orcid.org/0000-0003-4165-8100>
 Guangyu Wang  <https://orcid.org/0000-0003-0977-1453>
 Tongli Wang  <https://orcid.org/0000-0002-9967-6769>
 Jer-Ming Hu  <https://orcid.org/0000-0003-2739-9077>

REFERENCES

- Attorre, F., Alfò, M., Sanctis, M., Francesconi, B., Valenti, R., Vitale, M., & Bruno, F. (2011). Evaluating the effects of climate change on tree species abundance and distribution in the Italian peninsula. *Applied Vegetation Science*, 14, 242–255. <https://doi.org/10.1111/j.1654-109X.2010.01114.x>
- Bailey, R. G. (1983). Delineation of ecosystem regions. *Environmental Management*, 7, 365–373. <https://doi.org/10.1007/BF01866919>
- Barnes, B. V., Zak, D. R., Denton, S. R., & Spurr, S. H. (1997). *Forest ecology*, 4th ed. (p. 774). New York, NY: John Wiley & Sons Inc.
- Beckage, B., Osborne, B., Gavin, D. G., Pucko, C., Siccama, T., & Perkins, T. (2008). A rapid upward shift of a forest ecotone during 40 years of warming in the Green Mountains of Vermont. *Proceedings of the National Academy of Sciences of the United States of America*, 105, 4197–4202. <https://doi.org/10.1073/pnas.0708921105>
- Beniston, M. (2003). Climatic change in mountain regions: A review of possible impacts. *Climatic Change*, 59, 5–31. <https://doi.org/10.1023/A:1024458411589>
- Breiman, L. (2001). Random forests. *Machine Learning*, 45, 5–32. <https://doi.org/10.1023/A:1010933404324>
- Brinkmann, K., Patzelt, A., Schlecht, E., & Buerkert, A. (2011). Use of environmental predictors for vegetation mapping in semi-arid mountain rangelands and the determination of conservation hotspots. *Applied Vegetation Science*, 14, 17–30. <https://doi.org/10.1111/j.1654-109X.2010.01097.x>
- Chang, L.-M. (1974). Ecological studies on the vegetation of eastern coastal area of Taiwan. *Quarterly Journal of Chinese Forestry*, 7, 115–131 [In Chinese].
- Chao, W.-C., Chao, K.-J., Song, G.-Z.-M., & Hsieh, C.-F. (2007). Species composition and structure of the lowland subtropical rainforest at Lanjenchi, southern Taiwan. *Taiwania*, 52, 253–269.
- Chao, W.-C., Song, G.-Z.-M., Chao, K.-J., Liao, C.-C., Fan, S.-W., Wu, S.-H., ... Hsieh, C.-F. (2010). Lowland rainforests in southern Taiwan and Lanyu, at the northern border of Paleotropics and under the influence of monsoon wind. *Plant Ecology*, 210, 1–17. <https://doi.org/10.1007/s11258-009-9694-0>
- Chen, C., Liaw, A., & Breiman, L. (2004). *Using random forest to learn imbalanced data*. Berkeley, CA: University of California. Retrieved from <https://statistics.berkeley.edu/sites/default/files/tech-reports/666.pdf>
- Chiou, C.-R., Song, G.-Z.-M., Chien, J.-H., Hsieh, C.-F., Wang, J.-C., Chen, M.-Y., ... Chen, T.-Y. (2010). Altitudinal distribution patterns of plant species in Taiwan are mainly determined by the northeast monsoon rather than the heat retention mechanism of Massenerhebung. *Botanical Studies*, 51, 89–97.
- Chiu, C.-A., Chen, T.-Y., Wang, C.-C., Chiou, C.-R., Lai, Y.-J., & Tsai, C.-Y. (2013). Using BIOMOD2 to model the species distribution of *Fagus hayatae*. *Quarterly Journal of Forest Research*, 35, 253–272 [In Chinese with English summary].
- Evans, P., & Brown, C. D. (2017). The boreal-temperate forest ecotone response to climate change. *Environmental Reviews*, 25, 423–431. <https://doi.org/10.1139/er-2017-0009>
- Fang, J.-Y., Song, Y.-C., Liu, H.-Y., & Piao, S.-L. (2002). Vegetation-climate relationship and its application in the division of vegetation zone in China. *Acta Botanica Sinica*, 44, 1105–1122.
- Genauer, R., Poggi, J. M., & Tuleau-Malot, C. (2015). VSURF: An R package for variable selection using random forests. *The R Journal*, 7(2), 19–33. <https://doi.org/10.32614/RJ-2015-018>
- Hannaway, D. B., Daly, C., Cao, W. X., Luo, W. H., Wei, Y. R., Zhang, W. L., ... Li, L. X. (2005). Forage species suitability mapping for China using topographic, climatic and soils spatial data and quantitative plant tolerances. *Agricultural Science in China*, 4, 660–667.
- Hansen, A. J., & Phillips, L. B. (2015). Which tree species and biome types are most vulnerable to climate change in the US Northern Rocky Mountains? *Forest Ecology and Management*, 338, 68–83. <https://doi.org/10.1016/j.foreco.2014.11.008>
- Harris, I., Jones, P. D., Osborn, T. J., & Lister, D. H. (2014). Updated high-resolution grids of monthly climatic observations-the CRU TS 3.10 dataset. *International Journal of Climatology*, 34, 623–642. <https://doi.org/10.1002/joc.3711>
- Hengl, T., Walsh, M. G., Sanderman, J., Wheeler, I., Harrison, S. P., & Prentice, I. C. (2018). Global mapping of potential natural vegetation: An assessment of machine learning algorithms for estimating land potential. *PeerJ*, 6, e5457. <https://doi.org/10.7717/peerj.5457>
- Hijmans, R. J., Cameron, S. E., Parra, J. L., Jones, P. G., & Jarvis, A. (2005). Very high resolution interpolated climate surface for global land areas. *International Journal of Climatology*, 25, 1965–1978. <https://doi.org/10.1002/joc.1276>
- Holdridge, L. R. (1947). Determination of world plant formations from simple climatic data. *Science*, 105, 367–368. <https://doi.org/10.1126/science.105.2727.367>
- Holland, M. M., & Risser, P. G. (1991). Introduction: The role of landscape boundaries in the management and restoration of changing environments. In M. M. Holland, P. G. Risser, & R. J. Naiman (Eds.), *Ecotone: The role of landscape boundaries in the management and restoration of changing environments* (pp. 1–7). New York, NY, USA: Chapman & Hall.
- Hsieh, C.-F., Shen, C.-F., & Yang, K.-C. (1994). Introduction to the flora of Taiwan, 3: Floristics, phytogeography, and vegetation. In Huang & Editorial Committee of the Flora of Taiwan (Eds.), *Flora of Taiwan* (2nd ed., pp. 7–18). Taipei: Editorial Committee of the Flora of Taiwan.
- Hsu, H.-H., Chou, C., Wu, Y.-C., Lu, M.-M., Chen, C.-T., & Chen, Y.-M. (2011). *Climate change in Taiwan: Scientific report 2011 (Summary)*. Taipei, Taiwan: National Science Council.
- Klassen, H. A., & Burton, P. J. (2015). Climatic characterization of forest zones across administrative boundaries improves conservation planning. *Applied Vegetation Science*, 18, 343–356. <https://doi.org/10.1111/avsc.12143>
- Li, C.-F., Chytrý, M., Zelený, D., Chen, M.-Y., Chen, T.-Y., Chiou, C.-R., ... Hsieh, C.-F. (2013). Classification of Taiwan forest vegetation. *Applied Vegetation Science*, 16, 698–719. <https://doi.org/10.1111/avsc.12025>
- Liaw, A., & Wiener, M. (2002). Classification and regression by random Forest. *R News*, 2(3), 18–22.
- Lin, C.-T., Li, C.-F., Zelený, D., Chytrý, M., Nakamura, Y., Chen, M.-Y., ... Chiou, C.-R. (2012). Classification of the high-mountain coniferous forests in Taiwan. *Folia Geobotanica*, 47, 373–401. <https://doi.org/10.1007/s12224-012-9128-y>
- Lin, C.-Y., Lung, S.-C.-C., Guo, H.-R., Wu, P.-C., & Su, H.-J. (2009). Climate variability of cold surge and its impact on the air quality of Taiwan. *Climatic Change*, 94, 457–471. <https://doi.org/10.1007/s10584-008-9495-9>
- Lin, H.-Y., Hu, J.-M., Chen, T.-Y., Hsieh, C.-F., Wang, G., & Wang, T. (2018). A dynamic downscaling approach to generate scale-free regional climate data in Taiwan. *Taiwania*, 63, 245–266. <https://doi.org/10.6165/tai.2018.63.251>
- Liu, T.-S., & Su, H.-J. (1972). Synecological survey on the summer-green forest of north Chia-Tien Mountains. *Bulletin of Taiwan Museum*, 15, 1–16 [In Chinese].
- Martin, P. H., Sherman, R. E., & Fahey, T. J. (2007). Tropical montane forest ecotones: Climate gradients, natural disturbance,

- and vegetation zonation in the Cordillera Central, Dominican Republic. *Journal of Biogeography*, 34, 1792–1806. <https://doi.org/10.1111/j.1365-2699.2007.01726.x>
- Matsui, T., Nakao, K., Higa, M., Tsuyama, I., Kominami, Y., Yagihashi, T., ... Tanaka, N. (2018). Potential impact of climate change on canopy tree species composition of cool-temperate forests in Japan using a multivariate classification tree model. *Ecological Research*, 33, 289–302. <https://doi.org/10.1007/s11284-018-1576-2>
- Neilson, R. P. (1993). Transient ecotone response to climatic change: Some conceptual and modelling approaches. *Ecological Applications*, 3, 385–395. <https://doi.org/10.2307/1941907>
- Pearson, R. G., & Dawson, T. P. (2003). Predicting the impacts of climate change on the distribution of species: Are bioclimate envelope models useful? *Global Ecology & Biogeography*, 12, 361–371. <https://doi.org/10.1046/j.1466-822X.2003.00042.x>
- Rehfeldt, G. E., Crookston, N. L., Sáenz-Romero, C., & Campbell, E. M. (2012). North American vegetation model for land-use planning in a changing climate: A solution to large classification problems. *Ecological Applications*, 22, 119–141. <https://doi.org/10.1890/11-0495.1>
- Rehfeldt, G. E., Crookston, N. L., Warwell, M. V., & Evans, J. S. (2006). Empirical analyses of plant-climate relationships for the western United States. *International Journal of Plant Sciences*, 167, 1123–1150. <https://doi.org/10.1086/507711>
- Risser, P. G. (1995). The status of the science examining ecotones. *BioScience*, 45, 318–325. <https://doi.org/10.2307/1312492>
- Sasaki, S. (1924). Vegetation zones of Sin-Kao Shan. *Report of Formosan Natural History Society*, 69, 1–54 [In Japanese].
- Su, H.-J. (1984a). Studies on the climate and vegetation types of the natural forests in Taiwan (I). Analysis of the variations in climatic factors. *Quarterly Journal of Chinese Forestry*, 17, 1–14.
- Su, H.-J. (1984b). Studies on the climate and vegetation types of the natural forests in Taiwan (II). Altitudinal vegetation zones in relation to temperature gradient. *Quarterly Journal of Chinese Forestry*, 17, 57–73.
- Su, H.-J. (1985). Studies on the climate and vegetation types of the natural forests in Taiwan (III). A scheme of geographical climatic regions. *Quarterly Journal of Chinese Forestry*, 18, 33–44.
- Suzuki, T. (1938). Associations of *Laurilignosa* in the watershed of Tong-Hou stream. *Japanese Journal of Ecology*, 4, 197–314 [In Japanese].
- Wang, T., Campbell, E. M., O'Neill, G. A., & Aitken, S. N. (2012). Projecting future distributions of ecosystem climate niches: Uncertainties and management applications. *Forest Ecology and Management*, 279, 128–140. <https://doi.org/10.1016/j.foreco.2012.05.034>
- Wang, T., Hamann, A., Spittlehouse, D., & Carroll, C. (2016). Locally downscaled and spatially customizable climate data for historical and future periods for North America. *PLoS ONE*, 11(6), e0156720. <https://doi.org/10.1371/journal.pone.0156720>
- Wang, T., Wang, G., Innes, J., Nitschke, C., & Kang, H. (2016). Climatic niche models and their consensus projections for future climates for four major forest tree species in the Asia-Pacific region. *Forest Ecology and Management*, 360, 357–366. <https://doi.org/10.1016/j.foreco.2015.08.004>
- Wang, T., Wang, G., Innes, J., Seely, B., & Chen, B. (2017). ClimateAP: An application for dynamic local downscaling of historical and future climate data in Asia Pacific. *Frontiers of Agricultural Science and Engineering*, 4, 448–458.
- Wasson, K., Woolfolk, A., & Fresquez, C. (2013). Ecotones as indicators of changing environmental conditions: Rapid migration of salt marsh-upland boundaries. *Estuaries and Coasts*, 36, 654–664. <https://doi.org/10.1007/s12237-013-9601-8>
- Weng, S.-P., & Yang, C.-T. (2012). The construction of monthly rainfall and temperature dataset with 1km gridded resolution over Taiwan area (1960–2009) and its application to climate projection in the near future (2015–2039). *Atmospheric Sciences*, 40, 349–369 [In Chinese with English summary].
- Whittaker, R. H. (1975). *Communities and Ecosystems*. New York, NY, USA: MacMillan Publishing.
- Zhang, L., Liu, S., Sun, P., Wang, T., Wang, G., Zhang, X., & Wang, L. (2015). Consensus forecasting of species distributions: The effects of niche model performance and niche properties. *PLoS ONE*, 10(3), e0120056. <https://doi.org/10.1371/journal.pone.0120056>
- Zhu, H., Yong, C., Zhou, S., Wang, H., & Yan, L. (2015). Vegetation, floristic composition and species diversity in a tropical mountain nature reserve in southern Yunnan, SW China, with implications for conservation. *Tropical Conservation Science*, 8, 528–546. <https://doi.org/10.1177/194008291500800216>

SUPPORTING INFORMATION

Additional supporting information may be found online in the Supporting Information section.

How to cite this article: Lin H-Y, Li C-F, Chen T-Y, et al. Climate-based approach for modeling the distribution of montane forest vegetation in Taiwan. *Appl Veg Sci*. 2020;00:1–15. <https://doi.org/10.1111/avsc.12485>